Long Non-Coding RNA Osr2 Promotes *Fusarium solani* Keratitis Inflammation via the miR-30a-3p/ Xcr1 Axis

Hanfeng Tang, Yi Lin, and Jianzhang Hu

Department of Ophthalmology, Fujian Medical University Union Hospital, Fu Zhou, China

Correspondence: Jianzhang Hu, The Department of Ophthalmology, Fujian Medical University Union Hospital, 29 Xinquan Road, Fuzhou 350005, China; ophhjz@163.com.

HT and YL contributed equally to this project and should be considered co-first authors.

Received: November 3, 2024
Accepted: March 3, 2025
Published: March 11, 2025

Citation: Tang H, Lin Y, Hu J. Long non-coding RNA Osr2 promotes *Fusarium solani* keratitis inflammation via the miR-30a-3p/ Xcr1 axis. *Invest Ophthalmol Vis Sci.* 2025;66(3):27. https://doi.org/10.1167/iovs.66.3.27

Purpose. Fungal keratitis (FK) is a challenging and sight-threatening corneal disease caused by fungal infections. Although long noncoding RNAs (lncRNAs) have been explored in various infectious diseases, their specific roles in FK remain largely unexplored.

Methods. A mouse model of FK was created by infecting corneal stromal cells with *Fusarium solani*. High-throughput lncRNA expression profiling was conducted on FK-affected corneal tissues to identify differentially expressed lncRNAs. Reverse transcription quantitative PCR (RT-qPCR) was used to validate the results. A competing endogenous RNA (ceRNA) network was constructed. Additionally, a specific antisense oligonucleotide (ASO) targeting lncRNA ENSMUST00000226838/Osr2 (Osr2) was developed for therapeutic evaluation. Inflammatory markers IL-1β, IL-6, and TNF-α were measured, and corneal inflammation was assessed through histological analysis and slit-lamp examination. Fluorescent in situ hybridization (FISH) was used to confirm Osr2 localization, whereas a dual-luciferase reporter assay verified interactions between Osr2 and miR-30a-3p.

Results. We identified 1143 differentially expressed lncRNAs in FK, with 701 upregulated and 442 downregulated. The ceRNA network analysis indicated that lncRNA Osr2 regulates Xcr1 expression through miR-30a-3p. Treatment with ASO-Osr2 significantly reduced corneal inflammation, and FISH confirmed lncRNA Osr2 distribution in both the nucleus and cytoplasm. Dual-luciferase assays demonstrated the interaction between Osr2 and miR-30a-3p, highlighting their potential roles in the progression of FK.

Conclusions. This study outlined the lncRNA expression profile in FK and established a ceRNA regulatory network, identifying lncRNA Osr2 as a crucial modulator of FK pathogenesis through its interaction with miR-30a-3p. These findings highlighted lncRNA Osr2 as a promising therapeutic target for the treatment of FK.

Keywords: fungal keratitis (FK), long noncoding RNA (lncRNA), competing endogenous RNA (ceRNA), lncRNA Osr2, miR-30a-3p

Fungal keratitis (FK) is a vision-threatening invasive fungal infection primarily caused by *Fusarium solani*. It is characterized by severe inflammation, corneal ulceration, and opacity.[1,2] The disease is often characterized by a protracted course and is challenging to treat, compounded by the absence of reliable early diagnostic methods. The inflammatory response can cause substantial corneal damage, leading to a greater risk of blindness compared with other corneal diseases. In severe cases, it may even require enucleation.[3] Currently, the pathogenesis of FK is not fully understood, and effective therapeutic options are limited. Identifying key molecular factors associated with the disease is crucial for enhancing our understanding of its underlying mechanisms and for developing targeted treatment strategies.

Traditionally, revealing transcriptional mechanisms has been essential for understanding disease heterogeneity. Although significant progress has been made in deciphering the transcriptional code of coding regions, important insights and scientific mysteries still exist within the more diverse category of non-coding RNAs.[4,5] Among these, long noncoding RNAs (lncRNAs) have attracted considerable attention as a class of linear noncoding RNAs, typically exceeding 200 nucleotides in length, that regulate gene expression at various levels, including transcriptional, post-transcriptional, and epigenetic, and play key roles in numerous cellular biological processes.[6,7] Furthermore, lncRNAs located in the cytoplasm can serve as competing endogenous RNAs (ceRNAs), acting as "molecular sponges" that sequester microRNAs (miRNAs) and thereby regulate miRNA-mediated gene silencing.[8,9] The miRNAs, a class of regulatory noncoding RNAs approximately 20 to 24 nucleotides in length, are critical components of gene regulation, exerting their effects through partial complementarity with target mRNA sequences.[10,11] In our previous studies, we found that fungal infections significantly modify the miRNA expression profile in corneal tissues. Notably, several miRNAs, including miR-665-3p, are involved in the progression of FK.[12–14] As the functions of lncRNAs become more clearly understood and their roles in various infectious diseases are increasingly explored, there has yet to be a study specifically examining lncRNAs in the context of FK,

particularly regarding ceRNA regulatory networks. Further investigation in this area could deepen our understanding of the noncoding RNA landscape in FK, addressing a critical gap in current knowledge and potentially revealing new therapeutic targets for treatment.

In this study, we analyzed the differential expression profile of lncRNAs in FK and constructed a regulatory network linking lncRNAs, miRNAs, and mRNAs. Our findings suggested that lncRNA Osr2 may function as a ceRNA by sponging miR-30a-3p, thereby influencing the pathogenesis and progression of FK. This research provided new insights into the molecular mechanisms underlying FK and offered potential avenues for therapeutic intervention.

Materials and Methods

Preparation of *Fusarium solani*

The *Fusarium solani* strain (AS 3.1829) used in this study was obtained from the China General Microbiological Culture Collection Center (CGMCC) in Beijing, China. The fungus was cultured on Sabouraud medium at 28°C for 5 days. After incubation, the conidia were harvested and diluted with sterile water to a final concentration of 1×10^8 CFU/mL, creating the conidial suspension for subsequent experiments.

Experimental Animals

We sourced BALB/C mice (6–8 weeks old, male mice) from Charles River Lab Biological Technology Co., Ltd. (Beijing, China). We confirmed the health of the mice's eyes through a slit-lamp examination. All procedures were carried out in accordance with the guidelines established by the Association for Research in Vision and Ophthalmology (ARVO). Before infecting the mice with *Fusarium solani*, we randomly divided them into three groups (n = 6 per group): ASO-NC (lncRNA Osr2 negative control, 200 umol/L, Ribobio, Guangzhou, China; lnc6N0000002-1-10), ASO-OSR2 (lncRNA Osr2 antisense oligonucleotide, 200 umol/L; lnc1CM001), and a control group (with 5 µL saline injected into the conjunctiva). After anesthetizing the mice, a microinjector was used to administer a 5 µL solution into the conjunctiva. All solutions were injected at the time of modeling and again 48 hours post-modeling.

We established the FK model following a standardized protocol[15]: we administered pentobarbital intraperitoneally at a dose of 50 mg/kg, and excised a 2.5 mm section of the corneal epithelium using an electric scraper. A full-thickness rat cornea was cut along the limbus, shaped into a 5 mm soft contact lens, and placed on the mouse cornea. We then sutured the eyelids with 5-0 silk thread and introduced 5 µL of fungal suspension into the conjunctival sac. After 24 hours, we removed the contact lenses and sutures. We conducted daily observations of the corneas and captured photographs using a slit-lamp microscope, and we harvested the corneas for further analysis at designated time points.

Clinical Scoring

To evaluate the severity of FK, a clinical scoring system ranging from 0 to 12 was implemented. Three factors were assessed: corneal opacity density, opacity area, and surface smoothness, each rated on a scale from 0 to 4. The total score from these assessments categorized FK severity as mild (0–5), moderate (6–9), or severe (10–12).

Hematoxylin and Eosin Staining

We collected corneas from different groups (n = 6 per group) and fixed them in 4% paraformaldehyde (Sigma-Aldrich, St. Louis, MO, USA) overnight. After fixation, we dehydrated the samples through a series of graded alcohols, then embedded them in paraffin, and sectioned them using an ultramicrotome. Then, 5-µm thick sections were cut. We dewaxed the paraffin sections with xylene, rehydrated them in graded alcohol, and rinsed them thoroughly. Then, the tissues were immersed in hematoxylin solution for 5 minutes, followed by eosin staining for 1 to 2 minutes. Finally, we examined the stained tissues using an optical microscope (Nikon, Tokyo, Japan).

LncRNA Expression Microarray Analysis

Corneas were collected from both the control and fungal infection groups (n = 6 per group). The individual tissue samples were preserved in EP tubes at −80°C for later analysis. The lncRNA expression profiling was performed by KangCheng Biotechnology Co. Total RNA was extracted from the corneas using TRIzol reagent (Invitrogen). The quantity and quality of the RNA were evaluated using a NanoDrop ND-1000 (Thermo Scientific, Waltham, MA, USA), with samples chosen based on an OD260/OD280 ratio ranging from 1.8 to 2.1. Subsequently, each RNA sample was amplified and transcribed into fluorescent complementary RNA (cRNA), which was then hybridized to the Arraystar Mouse LncRNA Microarray version 4.0. After washing and fixing the arrays, they were scanned using the Agilent Scanner G2505C system. GeneSpring GX version 12.1 was used for data normalization and processing. Differentially expressed lncRNAs (DELs) were selected based on a fold change threshold of ≥2 and a significance level of $P < 0.05$.

Construction of miRNA/Targets and ceRNA Network

We utilized bioinformatics approaches to develop an interaction network that includes DELs, miRNAs (DEmiRs), and genes (DEGs). Data on DEmiRs were collected from previously published studies,[13] and miRNA target predictions were performed using the miRanda and TargetScan tools, with manual alignment of miRNA and lncRNA sequences. The resulting network was visualized using Cytoscape version 3.8.2.

Quantitative RT-PCR

The extraction of RNA from mouse corneas was conducted following standard protocols.[12] Subsequently, we performed cDNA synthesis using the Thermo Scientific Revertaid First Strand cDNA Synthesis Kit (Thermo Scientific, Waltham, MA, USA), and quantitative real-time PCR (qRT-PCR) was executed with ChamQ Universal SYBR qPCR Master Mix (Vazyme Biotech Co., Ltd., Nanjing, China) on an Applied Biosystems 7500 Real-Time PCR System (Foster City, CA, USA). The primer sequences for the selected lncRNAs, mRNAs, and miRNAs are listed in the Table.

Investigative Ophthalmology & Visual Science

Table. Primers Used in This Study

Gene	Forward	Reverse
ENSMUST00000196993	TCCCCCATACGGGTATCCAT	CAGTGTGACTTTTCTTTCATTTGCA
ENSMUST00000182676	TGAAAACCGAGCTCTGTGGATA	TAGGACACCCCCTGCATGTC
ENSMUST00000226838	GCTGAGACGCTTGGGTTGTC	GCTTCGAAAGCAGTCAGAACTCT
NR-151496.1	GGCTTGACTTTCACTGCTGTGT	GGCTTGAGGCAAATGTTTTTG
NR-104575.1	TGCACGGGTGACCCAGATAT	ATGGACAATAGTACCAACTCCAGCTA
ENSMUST00000126460	AAGAACCATGAGGAGGAAATTACTG	CCGTGACTTCGGTCTTGCTTATC
ENSMUST00000144415	TATGCCCCAGCAGTGAAAGC	GTCCGTCAGAGCATCCAACA
ENSMUST00000126470	GACCCTGCTGCTTGAGCTTAA	CACGGTAGCAAACCCGTCAT
ENSMUST00000208858	CAGACAGATCGCACCTGCAT	GGAAAGATCGACGACCTCCAT
ENSMUST00000225857	AGCAACATCAACCTCTGTGGCT	CAACTCCATCGCTTGGGTAAAA
ENSMUST00000161231	CAGGAACATCCTCTCCAAGTTCA	CGGCCATTGGGAGCTTCT
ENSMUST00000135050	ATCTGCTCTTGCTGCGTCTCTA	TTTAGGCTCAGCATCTTGACACC
miR-30a-3p	CCCCTTTCAGTCGGATGTTTG	CCAGTGCAGGGTCCGAGGT
Xcr1	CAGAGTCAGATGCTCTCAGTATCCC	TGTTACCCACAAGGCTGAGGAG
IL-1β	CTTTCCCGTGGACCTTCCA	CTCGGAGCCTGTAGTGCAGTT
IL-6	ACCACTCCCAACAGACCTGTCT	CAGATTGTTTTCTGCAAGTGCAT
TNF-α	ACAAGGCTGCCCCGACTAC	TGGGCTCATACCAGGGTTTG
GAPDH	GCCACCCAGAAGACTGTGGAT	GGAAGGCCATGCCAGTGA
U6	CTCGCTTCGGCAGCACA	AACGCTTCACGAATTTGCGT

Enzyme-Linked Immunosorbent Assay

The concentrations of IL-1β, IL-6, and TNF-α proteins were determined using ELISA kits sourced commercially, in accordance with the manufacturer's instructions (Mouse IL-1β, IL-6, and TNF-α ELISA kits from Proteintech, Wuhan, China). Absorbance values were measured with a multimode plate reader (Molecular Devices).

Luciferase Gene Reporter Assay

We synthesized the lncRNA Osr2 and the 3′ UTR of Xcr1, which included predicted miR-30a-3p binding sites and their corresponding mutant variants, and inserted them into pmiRRB-reporter vectors (RiboBio). We transfected the cells with either miR-30a-3p mimics or negative controls using Lipofectamine 3000 (Invitrogen). After 48 hours, we measured firefly and Renilla luciferase activities using the Dual-Luciferase Reporter Assay System (Promega Corporation, USA).

Primary Cell Culture

We thoroughly washed the isolated mouse eyeballs three times with sterile phosphate-buffered saline (PBS) containing penicillin and streptomycin (100 U/mL, TMS-AB2-C; Merck Millipore, Germany). Each eyeball was digested at 4°C for 12 hours using 150 µL of dispase II enzyme (15 mg/mL; Sigma, USA). After this, we carefully removed the loose corneal epithelium and minced the corneal tissues into small fragments. The fragments were then treated with collagenase A (10 mg/mL; Sigma, USA) at 37°C for 60 minutes. The resulting corneal stromal cells were suspended in DF12 medium (DMEM F-12; Sigma, USA) within a 25 cm^2 culture flask. We monitored the adherent cells after 12 hours of incubation at 37°C.

Fluorescence In Situ Hybridization of lncRNA

We employed a fluorescence in situ hybridization (FISH) kit (RiboBio) following the manufacturer's guidelines. First, we fixed the primary corneal stromal cells with 4% paraformaldehyde for 10 minutes at room temperature and then permeabilized them using 0.1% Triton X-100 for 5 minutes at 4°C. After washing the cells with PBS, we conducted RNA hybridization overnight at 37°C using Cy3-labeled probes targeting 18S, U6, and Osr2, ensuring protection from light. After hybridization, we rinsed the cells with SSC buffer (0.3 M NaCl and 0.03 M Na_3Citrate) at 42°C and stained the nuclei with DAPI. Finally, we performed fluorescence imaging using an LSM880 Zeiss inverted microscope (Carl Zeiss, Germany).

Statistical Analysis

All experiments were conducted independently at least three times. Fold change was calculated as the ratio of the mean values of the experimental and control groups. The combined error was determined by using the standard deviations of both groups to ensure accurate data representation. Reporting fold change values to two decimal places strikes a balance between precision and simplicity. Statistical analysis was performed using Student's *t*-test or 1-way ANOVA followed by Tukey's test, where appropriate, in GraphPad Prism version 8.0.1. A P value of less than 0.05 was considered statistically significant.

Results

Successfully Established a Mouse Model of FK

To investigate the pathological characteristics of FK, we established a mouse model. Our observations showed that the corneas began to exhibit increasing opacity and swelling as early as the first day post-infection, with a noticeable deterioration over time. By day 7, signs of resolution were evident (Fig. 1A). The hematoxylin and eosin (H&E) staining revealed significant epithelial defects and a marked accumulation of inflammatory cells, particularly prominent on day 5 after infection (Fig. 1B). Corneal congestion was apparent at the limbus on day 1, which progressed to corneal edema and neovascularization by day 3. By day 5, the tissue architecture was severely compromised, with localized ulcers or perforations emerging. However, by day 7, the severity

Investigative Ophthalmology & Visual Science

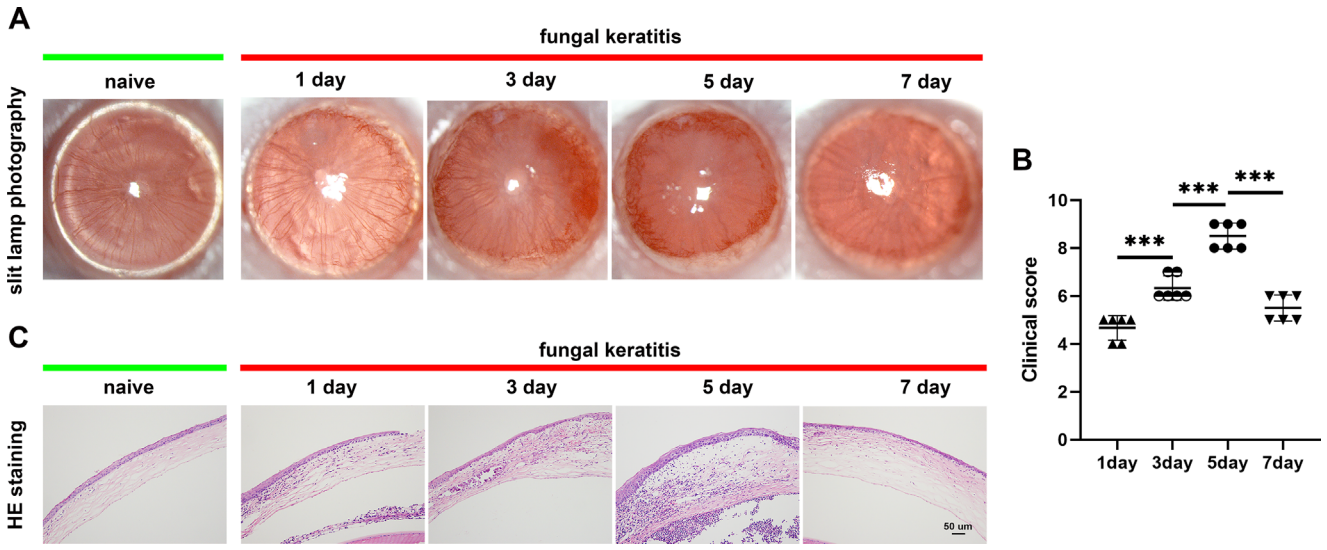

Figure 1. Clinical features in a mouse model of FK. (**A**) Slit-lamp images of corneal changes observed on days 1, 3, 5, and 7 following fungal infection. (**B**) Histopathological analysis of infected mouse corneas stained with H&E. Scale bar = 50 µm. (**C**) Clinical scoring indicates that inflammation peaked on day 5. Mice were allocated to control and fungal infection group ($n = 6$ per group). Data from three independent experiments. ***$P < 0.001$.

of the corneal infection had diminished, and scar healing was observed. These findings were reflected in the clinical scores, which corresponded with the observed pathological changes (Fig. 1C).

LncRNA Profiles in Corneal Tissues of Mice Following Fungal Infection

To further investigate the potential biological functions of lncRNAs in FK, we analyzed the lncRNA expression profiles in infected corneas compared with healthy controls. Using the Mouse LncRNA Array version 4.0 with 4 replicates per group, we identified a total of 33,124 lncRNA candidates. We discovered that 701 lncRNAs ($P < 0.05$, fold change ≥ 2) were significantly upregulated, whereas 442 were downregulated in the FK group compared with the healthy controls (Fig. 2A). Hierarchical clustering analysis clearly distinguished lncRNA expression patterns between the infected and control groups, emphasizing the impact of fungal infection on lncRNA regulation (Fig. 2B). We classified these lncRNAs by their genomic origin: 47% were exon sense-overlapping, 15% intergenic, 5% intron sense-overlapping, 9% intronic antisense, 19% natural antisense, and 5% bidirectional (Fig. 2C). Most lncRNAs had transcript lengths predominantly around 1000 nucleotides (Fig. 2D). Furthermore, we mapped the chromosomal distribution of all identified lncRNAs ($P < 0.05$) and the DELs, revealing specific chromosomal regions enriched in these DELs that may play a crucial role in the pathogenesis of FK (Fig. 2E).

Validation of Differentially Expressed lncRNAs by qRT-PCR

To confirm the reliability of the microarray data, we randomly selected 12 of the most significantly dysregulated lncRNAs for validation using qRT-PCR (Figs. 3A, 3B). The qRT-PCR results were consistent with the microarray findings, further supporting the identification of aberrantly expressed lncRNAs in FK mice models.

lncRNA-miRNA-mRNA Regulatory Network

We filtered lncRNAs that were predominantly localized in the cytoplasm using the lncATLAS database. Drawing from prior miRNA microarray data and mRNA transcriptome sequencing, we identified differentially expressed miRNAs and mRNAs associated with FK. Utilizing the TargetScan and miRanda algorithms, we constructed a ceRNA regulatory network that highlights the interactions among lncRNAs, miRNAs, and mRNAs. This network was visually represented using Cytoscape (Fig. 4).

Targeting lncRNA OSR2 Effectively Reduces Inflammation in FK

Antisense oligonucleotides (ASOs) have garnered significant interest for their ability to specifically target and degrade RNA, demonstrating efficacy in both in vitro and in vivo studies. Notably, following fungal infection, lncRNA OSR2 was found to be upregulated (fold change = 4.55 ± 0.14, $P < 0.001$) in corneal tissues compared to the control group. In response, we developed a targeted ASO (ASO-OSR2) and a negative control (ASO-NC) to assess their therapeutic potential in FK. Treatment with ASO-OSR2 resulted in a substantial reduction in corneal inflammation, as evidenced by decreased inflammatory cell infiltration confirmed through H&E staining (Fig. 5B). Clinical evaluations showed a significant reduction in scores in the ASO-OSR2 group compared to the ASO-NC group ($P < 0.001$; Fig. 5C), which was accompanied by a decrease in Xcr1 mRNA expression (Fig. 5D). Moreover, the levels of inflammatory cytokines IL-1β, IL-6, and TNF-α were significantly reduced at both mRNA and protein levels in the ASO-OSR2 group (Figs. 5E, 5F). Specifically, at the mRNA level, IL-1β was reduced (fold change = 4.70 ± 0.19, $P < 0.05$), IL-6 was reduced (fold change

Investigative Ophthalmology & Visual Science

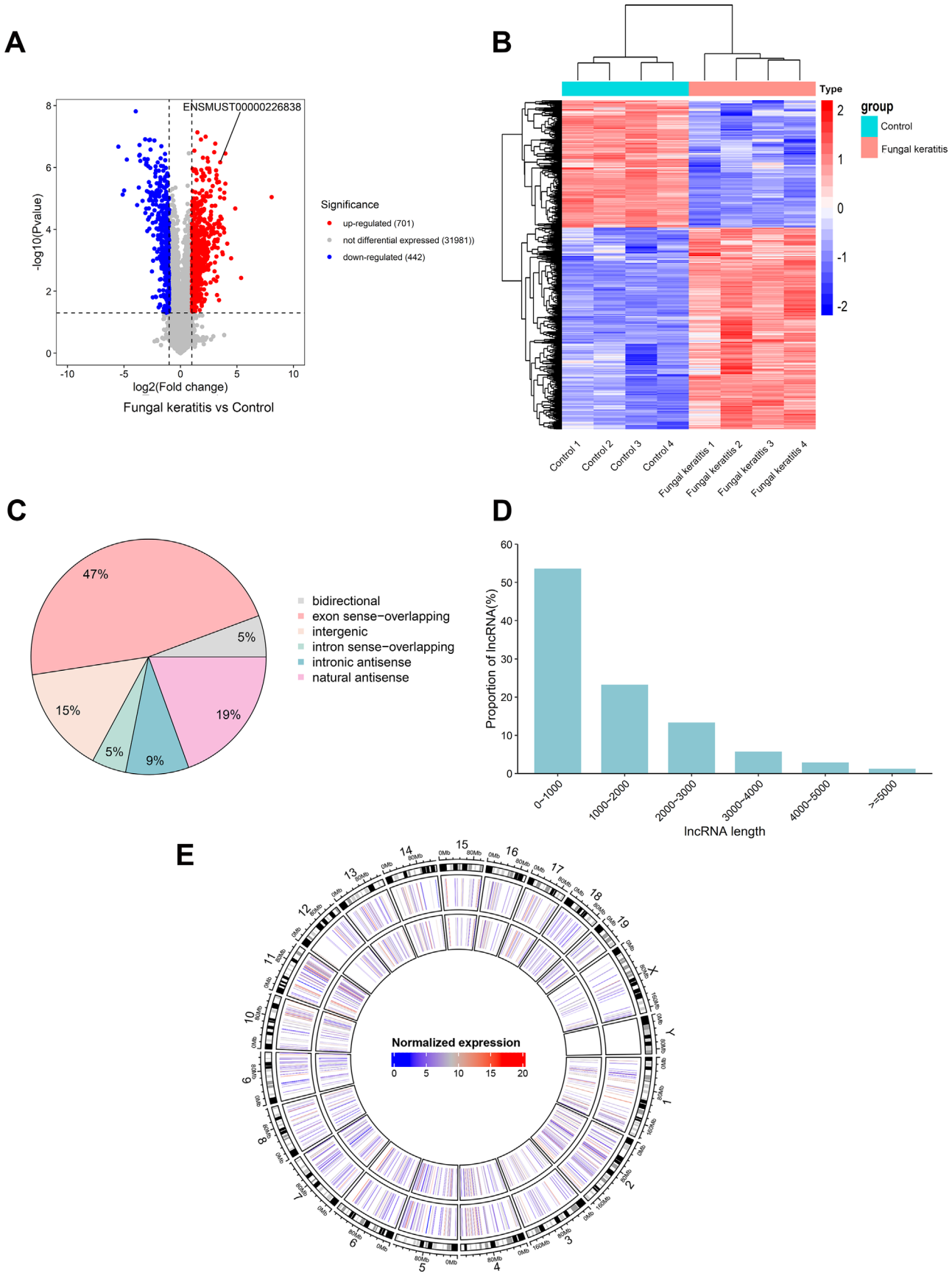

Figure 2. The lncRNA profiling in the FK and the control groups ($n = 6$ per group) using microarray analysis. (**A**) Volcano plot and (**B**) Hierarchical clustering analysis showing differentially expressed lncRNAs (DELs; fold change ≥ 2) between fungal keratitis and control groups. *Red* represents upregulated lncRNAs, whereas *green* denotes downregulation. (**C**) Classification of lncRNAs based on genomic

Investigative Ophthalmology & Visual Science

location. (**D**) Length distribution of lncRNA transcripts. (**E**) Chromosomal mapping of expressed lncRNAs ($P < 0.05$). The outermost ring shows mouse chromosomes, with inner layers representing expression patterns of all detected and differentially expressed lncRNAs.

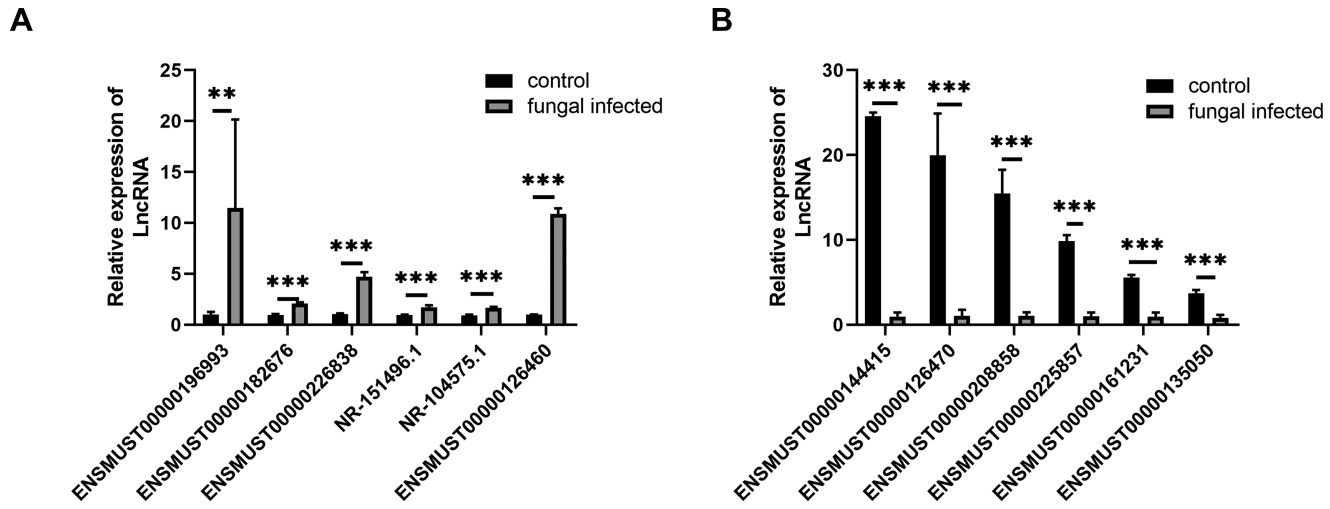

Figure 3. Validation of differentially expressed lncRNAs (DELs) identified by microarray analysis. (**A**) Validation of upregulated DELs and (**B**) downregulated DELs through qRT-PCR analysis, confirming the consistency with the microarray results. Data are presented as mean ± SD. Data from 3 independent experiments, each involving 12 pooled corneas, are presented, with significance levels indicated as $^{**}P < 0.01$ and $^{***}P < 0.001$.

= 8.12 ± 0.10, $P < 0.001$), and TNF-α was reduced (fold change = 1.90 ± 0.10, $P < 0.001$) in the ASO-OSR2 group compared to the control group. At the protein level, IL-1β was reduced (fold change = 1.90 ± 0.02, $P < 0.05$), IL-6 was reduced (fold change = 1.81 ± 0.02, $P < 0.05$), and TNF-α was reduced (fold change = 1.68 ± 0.01, $P < 0.01$) in the ASO-OSR2 group. These results indicate that suppressing lncRNA OSR2 can effectively alleviate FK symptoms and reduce inflammation.

LncRNA OSR2 Functions Through Targeting miR-30a-3p

In the current study, we have demonstrated that lncRNA OSR2 may play a role in the progression of FK. We selected the mechanism-related factor miR-30a-3p and found that its expression in corneal tissue decreased following fungal infection, whereas the expression of Xcr1 increased (Supplementary Fig. S1). To further elucidate the underlying mechanisms, we performed a dual-luciferase reporter assay. Our findings revealed that miR-30a-3p interacts with Xcr1. We created both wild-type and mutant Xcr1 luciferase reporter plasmids based on the predicted binding sites for miR-30a-3p (Fig. 6A). The dual-luciferase assay indicated that mutations at the binding site did not significantly affect luciferase activity (Fig. 6B). We also confirmed the interaction between lncRNA OSR2 and miR-30a-3p. Specifically, miR-30a-3p markedly decreased the luciferase activity of the WT-OSR2 construct, whereas mutation of the miR-30a-3p binding site on OSR2 eliminated this effect, demonstrating that lncRNA OSR2 directly binds to miR-30a-3p (Figs. 6C, 6D). Furthermore, the presence of WT-OSR2 significantly reversed the reduction in luciferase activity caused by miR-30a-3p in the wild-type Xcr1 reporter construct (fold change = 1.87 ± 0.30, $P < 0.01$; Fig. 6E). The FISH analysis showed that lncRNA OSR2 is localized in both the cytoplasm and nucleus (Fig. 6F). This localization further suggests that lncRNA OSR2 may function as a ceRNA by binding to miR-30a-3p, thereby playing a critical role in the pathogenesis of FK.

Discussion

In recent years, advancements in sequencing technologies have progressively illuminated the roles of lncRNAs, highlighting their involvement in various infectious disease mechanisms.[16–19] For instance, Wang et al. found that lncRNA-GM enhances IFN-I production and inhibits viral replication by promoting S-glutathionylation of TBK1, which reduces antiviral interferon levels and aids in viral immune evasion.[20] Additionally, following Listeria monocytogenes infection, macrophages can increase the expression of miR-1 to degrade lncSros1, resulting in the release of CAPRIN1. This process protects Stat1 mRNA, leading to elevated levels of STAT1 protein and ultimately enhancing IFN-γ signaling activation in macrophages, this, in turn, boosts the innate immune system's capacity to eliminate intracellular bacteria.[21] Despite growing insights into lncRNAs in infectious diseases, their roles in FK remain unexplored, creating a significant gap in understanding. Addressing this gap could lead to novel therapeutic targets for FK treatment. We initially established an FK model using BALB/C mice. Previous studies have shown that C57BL/6 mice exhibit more severe corneal inflammation following fungal infection, with an increased risk of corneal perforation.[22,23] In contrast, BALB/C mice exhibit a more moderate inflammatory response, which allows for easier observation and longitudinal monitoring of the corneal condition. Additionally, our research group has extensively studied the pathogenesis of fungal keratitis using BALB/C mice, enabling a more direct comparison with our previous findings.[12] This strain selection is consistent with the long-term research focus

Investigative Ophthalmology & Visual Science

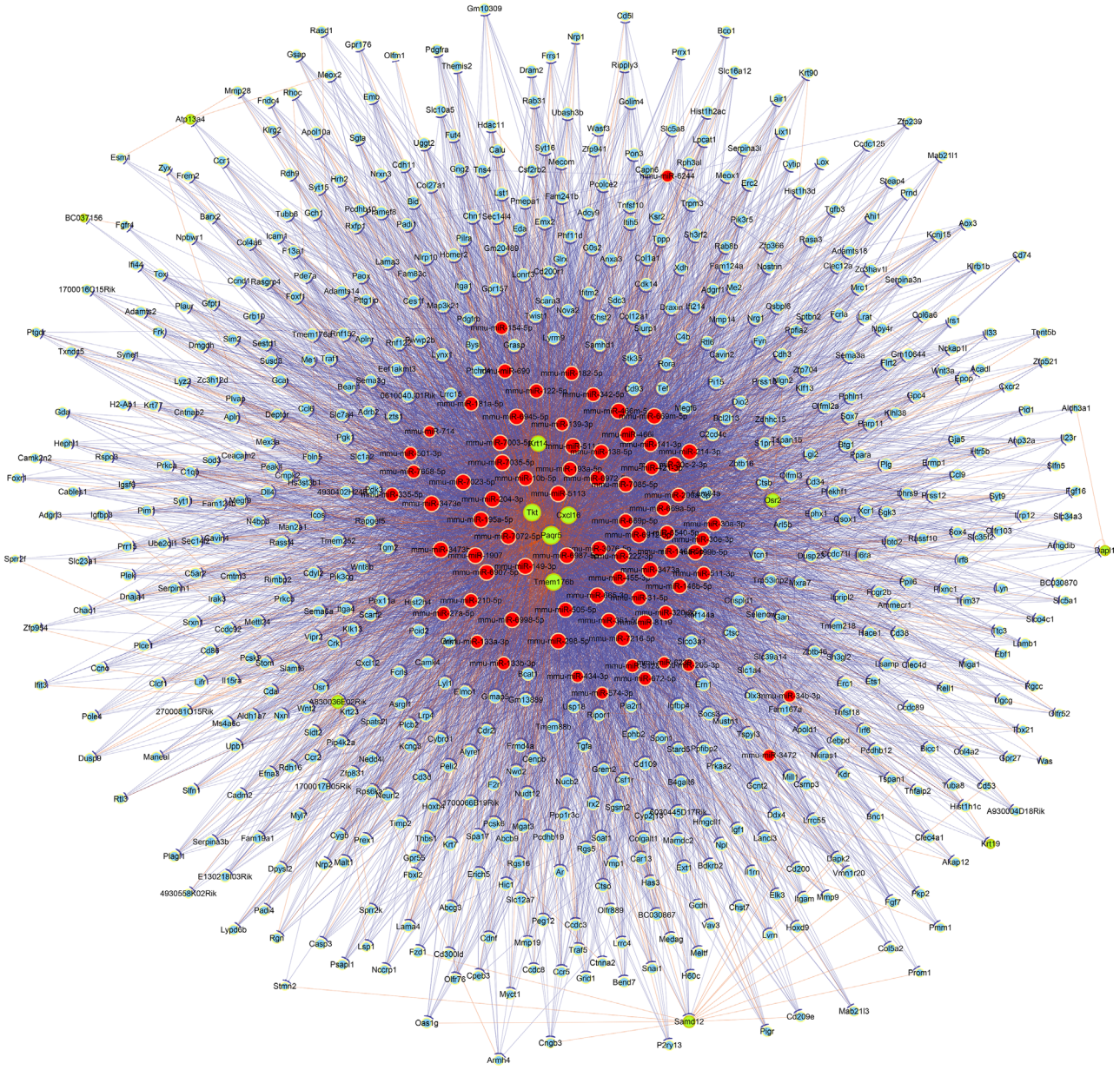

Figure 4. The ceRNA regulatory network in FK. The ceRNA network was constructed to illustrate the regulatory interactions among lncRNAs, miRNAs, and target genes relevant to fungal keratitis (FK). *Blue arrowheads* represent lncRNAs, *red ovals* indicate miRNAs, and *green hexagons* denote FK-associated target genes.

of our laboratory. We conducted high-throughput lncRNA microarray analysis to evaluate lncRNA expression profiles in corneal tissue following fungal infection, identifying 1143 significantly dysregulated lncRNAs (701 upregulated and 442 downregulated, with a fold change ≥ 2). Validation of selected dysregulated lncRNAs through qRT-PCR confirmed the reliability of our microarray results. By integrating previous transcriptome sequencing and miRNA chip data, we constructed a regulatory network that highlights the interactions among lncRNA, miRNA, and mRNA. Our further analysis focused on lncRNA OSR2, selected from the GENCODE database due to its high expression levels. PCR validation showed that lncRNA OSR2 was approximately upregulated (fold change $= 4.55 \pm 0.14$, $P < 0.001$) in corneal tissues compared to the control group. Our findings suggest that the lncRNA OSR2/miR-30a-3p/Xcr1 axis plays a significant role in corneal inflammation and the pathogenesis of FK.

ASO, is a short, chemically synthesized single-stranded oligonucleotide that effectively interferes with the expression of lncRNAs in both the nucleus and cytoplasm, as demonstrated by numerous studies highlighting its efficacy in vivo.[24–26] In our research, we used ASO to target lncRNA OSR2, and our findings showed that treatment with ASO-OSR2 significantly reduced inflammation in corneal tissue. This indicates that lncRNA OSR2 could serve as a promising therapeutic target for FK, although further investigation is needed to understand the specific mechanisms by which it modulates inflammation. Additionally, miRNAs play a criti-

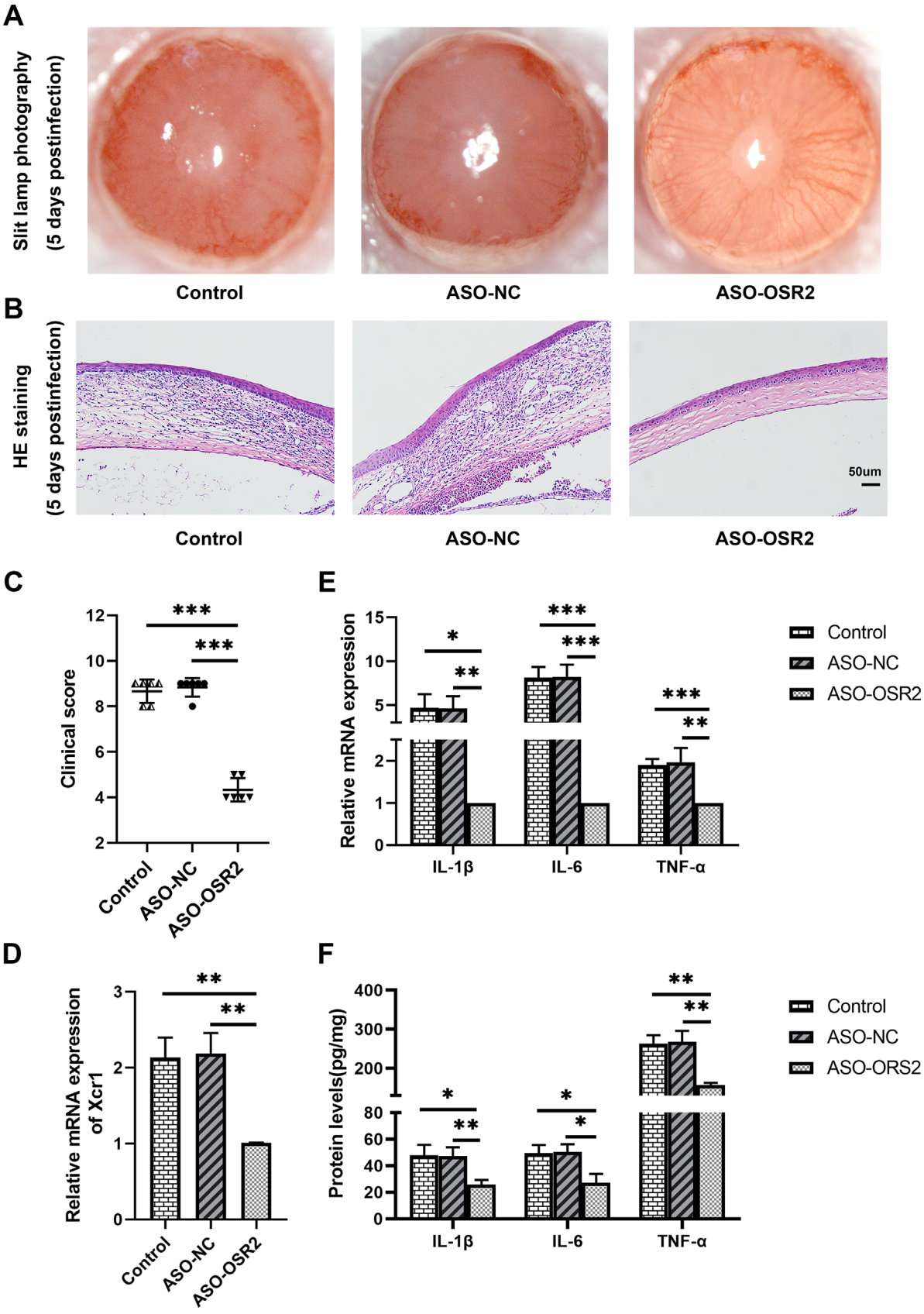

Figure 5. ASO-OSR2 treatment mitigates inflammation and improves clinical outcomes in FK. (**A**) Representative slit-lamp photographs of corneas 5 days post-infection ($n = 6$ per group). (**B**) Histopathological examination with H&E staining of mouse corneal tissues ($n = 6$ per group). Scale bar = 50 µm. (**C**) Clinical scoring demonstrated a significant reduction in inflammation in the ASO-OSR2 group compared to the ASO-NC group ($n = 6$ per group). (**D**) Expression levels of Xcr1 mRNA in each group ($n = 6$ per group). (**E, F**) Proinflammatory cytokine levels (IL-1β, IL-6, and TNF-α) were significantly decreased in the ASO-OSR2 group relative to the ASO-NC group ($n = 6$ per group). Data from 3 independent experiments, each with 12 pooled corneas, are summarized. $^{**}P < 0.01$, $^{***}P < 0.001$, and $^{****}P < 0.0001$.

Investigative Ophthalmology & Visual Science

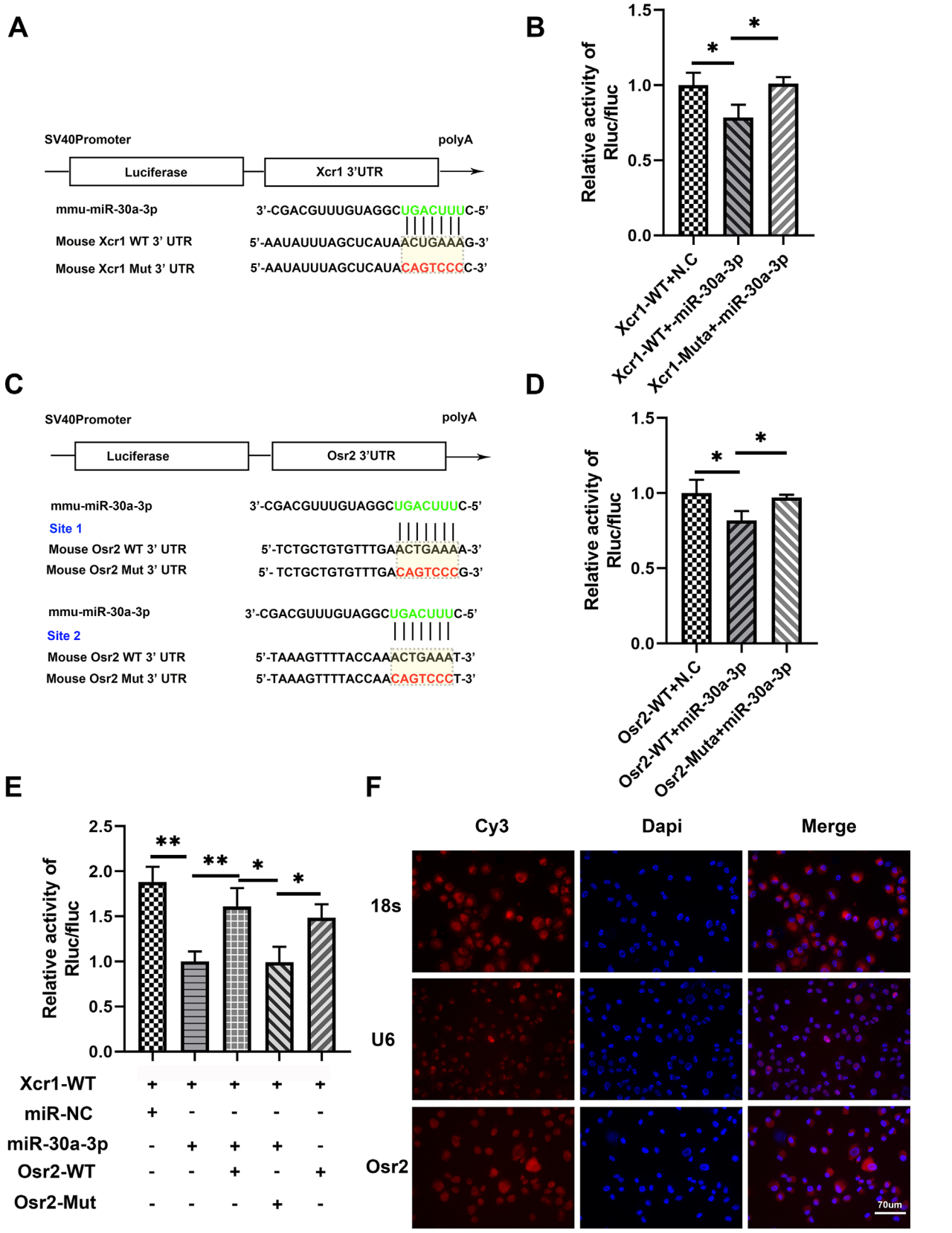

Figure 6. The lncRNA OSR2 serves as a miRNA sponge for miR-30a-3p, regulating Xcr1 expression. (**A**, **B**) Dual-luciferase reporter assays confirmed the interaction between miR-30a-3p and Xcr1, with both wild-type and mutant Xcr1 constructs tested. (**C**–**E**) Luciferase reporter assays demonstrated that miR-30a-3p binds directly to lncRNA OSR2, with mutations in the binding site reducing this interaction. (**F**) Fluorescence in situ hybridization (FISH) images show the localization of OSR2 (*red*) within corneal stromal cells, co-labeled with DAPI (*blue*). The 18S rRNA and U6 snRNA serve as cytoplasmic and nuclear controls, respectively. Data from three independent experiments. $^{*}P < 0.05$, $^{**}P < 0.01$.

Investigative Ophthalmology & Visual Science

cal role in post-transcriptional regulation by binding to the 3′ untranslated regions (UTRs) of various target mRNAs, affecting their stability and translation, and ultimately suppressing target protein synthesis.[27–29]

Our research team has conducted an extensive investigation into the role of miRNAs in FK. Using the Affymetrix Gene Chip miRNA 4.0 and bioinformatics analyses, we identified several differentially expressed miRNAs linked to the pathogenesis of fungal keratitis, with notable upregulation in several cases. In mouse models, miR-665-3p has been shown to regulate autophagy by targeting ATG5; inhibiting miR-665-3p enhanced autophagic activity and reduced inflammatory responses.[13] Additionally, suppressing miR-223-3p significantly increased the expression of autophagy-related proteins LC3-II in mouse corneal tissue, leading to a decrease in fungal burden and reduced immune cell infiltration. Bioinformatics analyses and luciferase reporter assays confirmed that miR-223-3p regulates autophagy by binding to the 3′ UTR of ATG16L1.[14] These findings underscore the important role of miRNAs in the progression of FK and highlight the need to explore upstream regulatory mechanisms to enhance our understanding of the expression profiles of relevant non-coding RNAs in this condition.

In our study, we observed a significant reduction in the expression of miR-30a-3p in FK (fold change = 0.56 ± 0.07, $P < 0.05$) in the experimental group, compared to the control group. The expression levels of its potential downstream target gene, Xcr1, were subsequently validated using qRT-PCR in vivo models. In LPS-induced human kidney 2 (HK-2) cells, downregulating miR-30a-3p appeared to enhance cell proliferation by targeting TEAD1, suggesting its potential as an early biomarker for sepsis-associated acute kidney injury.[30] Furthermore, miR-30a-3p has been identified as a crucial player in the survival mechanisms of *Mycobacterium* tuberculosis. Experimental findings indicate that Mycobacterium tuberculosis upregulates miR-30a-3p expression through its secreted early antigen target 6 (rESAT-6), which inhibits the autophagic process induced by calcineurin, thereby enhancing bacterial survival within macrophages, these observations highlight miR-30a-3p as a key regulatory factor in infectious diseases.[31]

The ceRNA regulatory network, a recently recognized mechanism of RNA interactions, has garnered significant attention since its introduction in 2011.[32] This framework posits that certain RNAs contain miRNA response elements (MREs) that compete for miRNA binding, thereby influencing miRNA regulation of mRNAs and affecting their translation at the post-transcriptional level. The lncRNAs can function as ceRNAs by acting like "sponges" that bind to miRNAs, reducing their inhibitory effects on target mRNAs and thus impacting disease progression.[33,34] The ceRNA mechanism provides a novel lens through which to explore miRNA-mediated epigenetic regulation. However, the role of lncRNA OSR2 as a ceRNA in the context of FK remains to be thoroughly investigated. Building on our previous findings, we hypothesize that lncRNA OSR2, a novel lncRNA, exhibits dysregulated expression in FK. Bioinformatics analyses suggest that it may function as a ceRNA for miR-30a-3p, playing a critical role in modulating the inflammatory response in this condition. To investigate the mechanisms involving lncRNA OSR2, we performed dual-luciferase reporter assays, which confirmed the interaction between Xcr1 and miR-30a-3p. We also identified a direct binding relationship between lncRNA OSR2 and miR-30a-3p; specifically, miR-30a-3p binding to the Xcr1 luciferase reporter inhibited its expression. Co-transfection of cells with an overexpression plasmid for lncRNA OSR2 restored luciferase activity, demonstrating that lncRNA OSR2 directly targets and binds to miR-30a-3p, thereby reversing its inhibitory effect on Xcr1. Furthermore, FISH experiments revealed that lncRNA OSR2 is widely distributed in both the nucleus and cytoplasm, highlighting its potential significance as a ceRNA in the pathogenesis of FK.

In conclusion, our results indicate that the lncRNA OSR2/miR-30a-3p/Xcr1 axis may be crucial in the development of FK. Inhibiting lncRNA OSR2 expression significantly reduces inflammation in corneal tissues after fungal infection, highlighting its potential as a valuable therapeutic target in clinical settings.

Acknowledgments

Supported by Joint Funds for the innovation of Science and Technology, Fujian province (Grant No. 2023Y9194 and 2020Y9060) and Fujian Provincial Natural Science Foundation of China (Grant No. 2024J01635).

Disclosure: **H. Tang**, None; **Y. Lin**, None; **J. Hu**, None

References

1. Brown L, Leck AK, Gichangi M, Burton MJ, Denning DW. The global incidence and diagnosis of fungal keratitis. *Lancet Infect Dis*. 2021;21(3):e49–e57.
2. Todokoro D, Suzuki T, Tamura T, et al. Efficacy of luliconazole against broad-range filamentous fungi including *Fusarium solani* species complex causing fungal keratitis. *Cornea*. 2019;38(2):238–242.
3. Szaliński M, Zgryźniak A, Rubisz I, Gajdzis M, Kaczmarek R, Przeździecka-Dołyk J. Fusarium keratitis—review of current treatment possibilities. *JCM*. 2021;10(23):5468.
4. Herman AB, Tsitsipatis D, Gorospe M. Integrated lncRNA function upon genomic and epigenomic regulation. *Mol Cell*. 2022;82(12):2252–2266.
5. Gonzales LR, Blom S, Henriques R, Bachem CWB, Immink RGH. LncRNAs: the art of being influential without protein. *Trends Plant Sci*. 2024;29(7):770–785.
6. Mattick JS, Amaral PP, Carninci P, et al. Long non-coding RNAs: definitions, functions, challenges and recommendations. *Nat Rev Mol Cell Biol*. 2023;24(6):430–447.
7. Nojima T, Proudfoot NJ. Mechanisms of lncRNA biogenesis as revealed by nascent transcriptomics. *Nat Rev Mol Cell Biol*. 2022;23(6):389–406.
8. Tay Y, Rinn J, Pandolfi PP. The multilayered complexity of ceRNA crosstalk and competition. *Nature*. 2014;505(7483):344–352.
9. Thomson DW, Dinger ME. Endogenous microRNA sponges: evidence and controversy. *Nat Rev Genet*. 2016;17(5):272–283.
10. Shang R, Lee S, Senavirathne G, Lai EC. microRNAs in action: biogenesis, function and regulation. *Nat Rev Genet*. 2023;24(12):816–833.
11. Ha M, Kim VN. Regulation of microRNA biogenesis. *Nat Rev Mol Cell Biol*. 2014;15(8):509–524.
12. Tang H, Lin Y, Huang L, Hu J. MiR-223-3p regulates autophagy and inflammation by targeting ATG16L1 in *Fusarium solani* –induced keratitis. *Invest Ophthalmol Vis Sci*. 2022;63(1):41.
13. Guo Q, Lin Y, Hu J. Inhibition of miR-665-3p enhances autophagy and alleviates inflammation in *Fusarium solani* -induced keratitis. *Invest Ophthalmol Vis Sci*. 2021;62(1):24.

14. Lin J, Lin Y, Huang Y, Hu J. Inhibiting miR-129-5p alleviates inflammation and modulates autophagy by targeting ATG14 in fungal keratitis. *Exp Eye Res*. 2021;211:108731.
15. Hu J, Wang Y, Xie L. Potential role of macrophages in experimental keratomycosis. *Invest. Ophthalmol. Vis. Sci*. 50:2087–2094.
16. Santus L, Sopena-Rios M, García-Pérez R, et al. Single-cell profiling of lncRNA expression during Ebola virus infection in rhesus macaques. *Nat Commun*. 2023;14(1):3866.
17. Runtsch MC, O'Neill LA. GOTcha: lncRNA-ACOD1 targets metabolism during viral infection. *Cell Res*. 2018;28(2):137–138.
18. Fitzgerald KA, Shmuel-Galia L. Lnc-ing RNA to intestinal homeostasis and inflammation. *Trends Immunol*. 2024;45(2):127–137.
19. Schmerer N, Schulte LN. Long noncoding RNAs in bacterial infection. *WIREs RNA*. 2021;12(6):e1664.
20. Munschauer M, Vogel J. Nuclear lncRNA stabilization in the host response to bacterial infection. *EMBO J*. 2018;37(13):e99875.
21. Wang P, Xu J, Wang Y, Cao X. An interferon-independent lncRNA promotes viral replication by modulating cellular metabolism. *Science*. 2017;358(6366):1051–1055.
22. Montgomery ML, Fuller KK. Experimental models for fungal keratitis: an overview of principles and protocols. *Cells*. 2020;9(7):1713.
23. Wu TG, Wilhelmus KR, Mitchell BM: Experimental keratomycosis in a mouse model. *Invest Ophthalmol Vis Sci*. 2003;44(1):210–216.
24. Wang Y, Wang P, Zhang Y, et al. Decreased expression of the host long-noncoding RNA-GM facilitates viral escape by inhibiting the kinase activity TBK1 via S-glutathionylation. *Immunity*. 2020;53(6):1168–1181.e7.
25. Xu H, Jiang Y, Xu X, et al. Inducible degradation of lncRNA Sros1 promotes IFN-γ-mediated activation of innate immune responses by stabilizing Stat1 mRNA. *Nat Immunol*. 2019;20(12):1621–1630.
26. Xiu B, Chi Y, Liu L, et al. LINC02273 drives breast cancer metastasis by epigenetically increasing AGR2 transcription. *Mol Cancer*. 2019;18(1):187.
27. Xin Z, Hu C, Zhang C, et al. LncRNA-HMG incites colorectal cancer cells to chemoresistance via repressing p53-mediated ferroptosis. *Redox Biology*. 2024;77:103362.
28. Lu TX, Rothenberg ME. MicroRNA. *J Allergy Clin Immunol*. 2018;141(4):1202–1207.
29. Kabekkodu SP, Shukla V, Varghese VK, D' Souza J, Chakrabarty S, Satyamoorthy K. Clustered miRNAs and their role in biological functions and diseases. *Biol Rev Camb Philos Soc*. 2018;93(4):1955–1986.
30. Su J, Wang Y, Xie J, et al. MicroRNA-30a inhibits cell proliferation in a sepsis-induced acute kidney injury model by targeting the YAP-TEAD complex. *J Intensive Med*. 2024;4(2):231–239.
31. Behura A, Mishra A, Chugh S, et al. ESAT-6 modulates Calcimycin-induced autophagy through microRNA-30a in mycobacteria infected macrophages. *J Infect*. 2019;79(2):139–152.
32. Salmena L, Poliseno L, Tay Y, Kats L, Pandolfi PP. A ceRNA hypothesis: the Rosetta Stone of a hidden RNA language? *Cell*. 2011;146(3):353–358.
33. Nemeth K, Bayraktar R, Ferracin M, Calin GA. Non-coding RNAs in disease: from mechanisms to therapeutics. *Nat Rev Genet*. 2024;25(3):211–232.
34. Sanchez-Mejias A, Tay Y. Competing endogenous RNA networks: tying the essential knots for cancer biology and therapeutics. *J Hematol Oncol*. 2015;8(1):30.